

# Tracking Femtosecond Laser Pulses in Space and Time

M. L. M. Balistreri,\* H. Gersen,\* J. P. Korterik, L. Kuipers,  
N. F. van Hulst†

**We show that the propagation of a femtosecond laser pulse inside a photonic structure can be directly visualized and tracked as it propagates using a time-resolved photon scanning tunneling microscope. From the time-dependent and phase-sensitive measurements, both the group velocity and the phase velocity are unambiguously and simultaneously determined. It is expected that this technique will find applications in the investigation of the local dynamic behavior of photonic crystals and integrated optical circuits.**

The propagation of ultrafast laser pulses plays an important role in many aspects of modern optical science. As the pulses get shorter, their spectral content and peak intensity increase, giving rise to phenomena such as self-phase modulation, soliton formation, and other nonlinear effects (1). With the appearance of advanced photonic structures, a new dimension has been added to the manipulation of light propagation (2), particularly the strong influence photonic crystals have on the propagation of pulses. The geometry of the structures leads to exciting phenomena such as the creation of gap solitons (3) or the occurrence of extremely short tunneling times (4, 5). In addition to the academic interest, pulse propagation is important in telecommunication applications where the above-mentioned effects can be either detrimental or beneficial for information transport via fiber networks. It is therefore necessary that a clearer and more complete understanding of ultrafast pulse propagation in advanced photonic structures be sought.

Conventionally, pulse propagation is studied with “black box”-type measurements: Pulses are coupled into the structure of interest, the transmitted or reflected light is collected and analyzed with various auto- and cross-correlation techniques (1), and the results are then compared to a theoretical model. As the pulses are collected outside the structure of interest, little direct insight into the behavior of the pulses inside the structure is obtained. In order to obtain more insight into the propagation phenomena that develop throughout the structure, the experiment is usually repeated for different lengths of the structure (6), a procedure that has clear drawbacks. First, not every photonic structure can be arbitrarily changed in length without af-

fecting its properties. Second, when a conflict between experiment and theory is found, it may be hard to find the underlying cause for the discrepancy. Third, the method integrates all the pulse propagation effects accumulated in the entire structure. If a structure has spatially varying optical properties, only averaged information is obtained. To overcome these drawbacks, a nondestructive method is necessary for the investigation of pulse propagation en route: a method that can track, visualize, and characterize pulses as they propagate through the structure.

Local optical measurements with a resolution beyond the diffraction limit are possible with a near-field optical microscope (7). With this scanning probe technique [hereafter called a photon scanning tunneling microscope (PSTM)] in collection mode, the local intensity distributions of light inside a photonic structure can be mapped with subwavelength resolution (8). Near-field optical microscopy has proven a powerful technique for measuring local intensity distributions of light inside photonic structures of varying complexity, where various unexpected optical phenomena were discovered, and the behavior of complex structures could be elucidated (9–11). Recently, not only the local intensity distributions have been mapped but also the local evolution of the phase of the propagating light (12, 13). These optical phase measurements resulted in the visualization of phase singularities in the plane of propagation (12). Typically, resolutions attainable with a PSTM are  $\sim 50$  nm (7–12) and better (13). However, in all cases the steady-state behavior of the light propagation is visualized. Until now, time-resolved near-field optical microscopy has focused on studies of single molecules (14) and carrier dynamics in nanostructures (15–17) rather than on light propagation.

Here we report a technique for tracking a femtosecond laser pulse as it propagates through a photonic structure. The instrument used is based on a recently developed hetero-

dyne detection phase-sensitive PSTM and can pinpoint the position in space of the propagating pulse at a particular point in time. By changing the reference point in time, the actual propagation of the pulse can be visualized. Because the measurement is both phase-sensitive and time-resolved, it allows measurement of all properties of the light pulse as it propagates, in particular its phase and group velocity.

In the PSTM, the local evanescent field above a photonic structure is picked up with a subwavelength fiber probe (18). The evanescent field is locally converted into a propagating wave that is subsequently detected. The evanescent field above the structure is associated with a propagating wave inside the structure. In a plane perpendicular to the propagation direction, the evanescent field and the propagating wave have the same phase and time information. By picking up the evanescent field, direct information is obtained on the propagating light field (19). By raster scanning the probe over the sample surface while keeping the sample-probe distance constant, the topography of the sample is measured simultaneously with the optical information (Fig. 1). The pulses are launched into the structure, where they propagate. At a certain position, a near-field optical probe is used to pick up a tiny fraction of the pulse. This signal is then interferometrically mixed with a laser pulse that is split off from the same laser source and has propagated along the reference branch of the setup. The interference between light in the signal and reference branches is then measured with a photomultiplier tube. Heterodyne detection is established by acousto-optical modulation in the reference branch of the interferometer, enabling a separation of amplitude and phase information from the measured interference fringes with a dual-output lock-in amplifier (19). An optical delay line in the reference branch completes the pulse tracking setup. The position of the optical delay line determines the length of the reference branch. Optical interference will only occur when there is temporal overlap between the pulses in the signal and the reference branch at the point where the branches join again. In effect, each position of the optical delay defines a certain reference time  $\tau$ . For a given location of the probe, the measured interference is determined by the cross-correlation  $\Xi(\tau) = \int dt E_{\text{sig}}(t) E_{\text{ref}}^*(t - \tau)$ , between the two time-dependent optical fields  $E_{\text{sig}}(t)$  and  $E_{\text{ref}}(t)$  in the signal and the reference branch, respectively, as a function of the reference time  $\tau$ . As the fiber probe is scanned across the photonic structure, any interference detected at a specific fiber position indicates that at that reference time, the pulse has traveled to that location. As a result, the center of the pulse can be followed in time.

Applied Optics group, Department of Applied Physics and MESA<sup>+</sup> Research Institute, University of Twente, Post Office Box 217, 7500 AE Enschede, Netherlands.

\*These authors contributed equally to this work.

†To whom correspondence should be addressed. E-mail: N.F.vanHulst@tn.utwente.nl

## REPORTS

As a model system for the pulse tracking experiment we have used a silicon nitride planar channel waveguide with femtosecond laser pulses generated from a frequency-doubled Ti:sapphire-pumped optical parametric oscillator. Nearly bandwidth-limited laser pulses with a pulse duration of  $300 \pm 20$  fs [center wavelength ( $\lambda_{\text{center}}$ ) = 632 nm], are launched into the waveguide with the polarization of light perpendicular to the sample plane, such that only the TM mode is excited. In the measured topography of the waveguide structure (Fig. 2A), obtained simultaneously with the optical information, the  $2.0 \pm 0.3$  nm-high ridge is clearly resolved. Measured optical amplitudes of five pulse measurements for increasing reference times are shown (Fig. 2, B through F) where, for each reference time, a roughly Gaussian amplitude envelope of interference is found that reveals the position of the pulse, thereby pinpointing

the pulse position for each reference time. As time passes, the pulse is found further down the waveguide; it is tracked while it propagates. The speed at which the pulse envelope propagates (the group velocity) is determined from the positional change of the “center of mass” of the pulse during the known time interval. Between each measurement, the reference time is shifted  $133 \pm 2$  fs by lengthening the reference branch by  $40.0 \pm 0.6$   $\mu\text{m}$ . The linear dependence of the position of the pulse in the waveguide as a function of the reference time (Fig. 3) shows that the pulse propagates locally with a constant group velocity. From the slope of the fitted straight line, we find a group velocity of  $1.67 \pm 0.03 \times 10^8$  m/s, in good agreement with a calculated value of  $1.69 \pm 0.08 \times 10^8$  m/s for the locally measured waveguide geometry (20).

For each pulse measurement, an optical

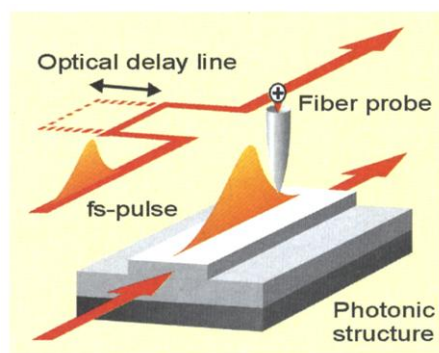


**Fig. 1.** Schematic representation of a pulse tracking experiment. The evanescent field of the pulse traveling inside the waveguide is picked up by a subwavelength near-field optical probe. The signal that is picked up is then interferometrically recombined with the pulse in a reference branch. The length of the reference branch, and thus the time that it takes the reference pulse to travel in this branch, is controlled with an optical delay line. The near-field optical probe is scanned across the photonic structure while its height above the structure is kept constant. The photonic sample is a ridge waveguide. The waveguide was fabricated in a  $\text{SiO}_2/\text{Si}_3\text{N}_4$  layer system on Si. The measured height and width of the channel ridge are  $2.0 \pm 0.3$  nm and  $2.86 \pm 0.09$   $\mu\text{m}$ . The slab thickness is determined to be  $124 \pm 5$  nm. Three guided modes can be excited in the waveguide [two transverse electric (TE) and one transverse magnetic (TM) polarized modes].

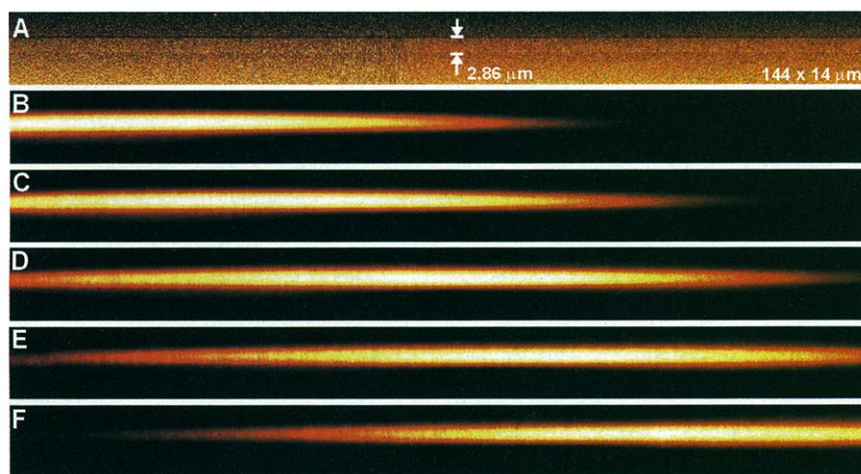


**Fig. 2.** False color representation of a pulse tracking measurement (image size:  $144 \times 14$   $\mu\text{m}^2$ ) (A) The topography of the photonic structure as measured with the height regulation. The ridge waveguide is clearly visible. (B through F) The optical field amplitude as measured by the instrument for different positions of the optical delay line. From (B) through (F), the optical path length of the reference branch is increased by  $40.0 \pm 0.6$   $\mu\text{m}$ . This results in steps of the reference time of  $133 \pm 2$  fs. The measurement shows that the position of the pulse at a reference time can be pinpointed in space. The pulses can be seen to propagate through the structure as a function of time.

phase image is obtained together with the amplitude data. Figure 4 displays the combined phase and amplitude information at a fixed reference time, corresponding to zero delay in Fig. 3. The pattern in Fig. 4A clearly shows the envelope and the fringes for a single scan line along the propagation direction, whereas the high-resolution spatial map (Fig. 4B) reveals the plane wavefront within the pulse. A simple Fourier transform of the data suffices to determine which central wavelengths are contained in the fringe pattern. We find a central wavelength of  $415 \pm 6$  nm. This wavelength corresponds to a phase velocity of  $1.97 \pm 0.03 \times 10^8$  m/s, which is close to a calculated value of  $2.02 \pm 0.02 \times 10^8$  m/s for the structure under study (20).

The measured envelope shows a roughly Gaussian shape with a length of 80.4  $\mu\text{m}$ . The envelope is also found to be a little asymmetric: It has a slightly sharper rising edge (long distances corresponding to short times in the pulse) and a tail that falls off more slowly. The observed asymmetry and the effective length of the envelope are explained by the fact that the pulse has undergone different group velocity dispersion in both the reference and the signal branch (21). As a result, the pulses have different chirps when recombined, resulting in the asymmetric envelope.

It is tempting to consider the information presented as a cross-correlation of the optical fields in the reference branch and the photonic structure. However, this notion is incorrect (22). The measured signal does contain the local spectral content of the light inside the structure via the measured fringes. In addition, the signal contains information on the dispersion as it occurs on the length scale of the actual scan ( $\sim 150$   $\mu\text{m}$ ). In our instrument, we do have the ability to measure the above-mentioned cross-correlation as a function of position. To this end, the near-field

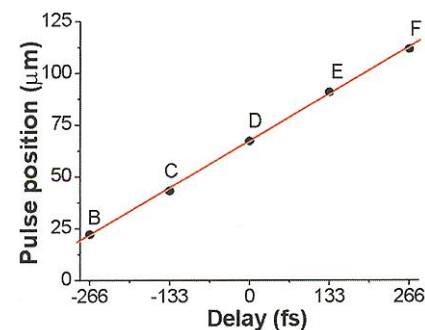


**Fig. 3.** Measured position of the pulse as a function of the position of the delay line (solid circles). The solid straight line represents a least-squares fit to the measured points. The slope of the line yields a group velocity for the pulse inside the photonic structure of  $1.67 \pm 0.03 \times 10^8$  m/s.

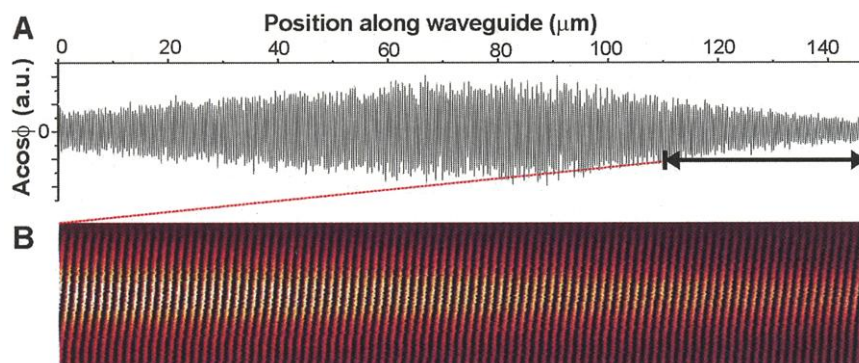


**Fig. 4.** (A) The optical amplitude  $A$  times the cosine of the optical phase  $\cos\phi$  for a single tracked pulse as measured through the heart of the waveguide for the entire scan range (Fig. 2D). a.u., arbitrary units. A clear fringe pattern with an envelope is observed. The envelope is slightly asymmetric owing to the different chirps of the signal and reference pulses. (B) False color representation of  $A\cos\phi$  as a function of the lateral position in the plane of the sample. The area depicted is an enlargement of a small part of the actual scan; the location is indicated by the double arrow in (A). It is clear that the wavefronts in the image are straight, indicating plane wave propagation. The periodicity of the wavefronts yields the wavelength inside the structure associated with the central optical frequency of the spectrum of the femtosecond laser pulse. The wavelength is found to be  $415 \pm 6$  nm, corresponding to a phase velocity of  $1.97 \pm 0.03 \times 10^8$  m/s.

probe is kept at a fixed location while the interference is measured as a function of the position of the optical delay line. In this way, it is even possible to measure the transmission function of a certain stretch of photonic structure by carrying out this procedure on either end of the stretch and comparing the results.

#### References and Notes

1. J.-C. Diels, W. Rudolph, *Ultrashort Laser Pulse Phenomena: Fundamentals, Techniques, and Applications on a Femtosecond Time Scale* (Academic Press, San Diego, CA, 1996).
2. *Photonic Crystals and Light Localization in the 21st Century*, C. M. Soukoulis, Ed. (NATO Science Series, Kluwer Academic, Dordrecht, Netherlands, 2001).
3. S. John, N. Aközbeç, *Phys. Rev. Lett.* **71**, 1168 (1993).
4. A. M. Steinberg, P. G. Kwiat, R. Y. Chiao, *Phys. Rev. Lett.* **71**, 708 (1993).
5. C. Spielmann, R. Szipöcs, A. Stingl, F. Krausz, *Phys. Rev. Lett.* **73**, 2308 (1994).
6. For a classical and powerful example, see K. Smith, L. F. Mollenauer, *Opt. Lett.* **14**, 1284 (1989).
7. E. Betzig, J. K. Trautman, T. D. Harris, J. S. Weiner, R. L. Kostelak, *Science* **251**, 1468 (1991).
8. R. C. Reddick, R. J. Warmack, T. L. Ferrel, *Phys. Rev. B* **39**, 767 (1989).
9. M. L. M. Balistreri *et al.*, *Opt. Lett.* **24**, 1829 (1999).
10. J. R. Krenn *et al.*, *Phys. Rev. Lett.* **82**, 2590 (2000).
11. S. I. Bozhevolnyi, J. Erland, K. Leosson, P. M. W. Skovgaard, J. M. Hvam, *Phys. Rev. Lett.* **86**, 3008 (2001).
12. M. L. M. Balistreri, J. P. Korterik, L. Kuipers, N. F. van Hulst, *Phys. Rev. Lett.* **85**, 294 (2000).
13. A. Nesci, R. Dändliker, H. P. Herzig, *Opt. Lett.* **26**, 208 (2001).
14. X. S. Xie, R. C. Dunn, *Science* **265**, 361 (1994).
15. V. Emiliani, T. Günther, C. Lienau, R. Notzel, K. H. Ploog, *Phys. Rev. B* **61**, 10583 (2000).
16. M. Achermann *et al.*, *Appl. Phys. Lett.* **76**, 2695 (2000).
17. J. R. Guest *et al.*, *Science* **293**, 2224 (2001).
18. For a recent review, see J. W. P. Hsu, *Mat. Sci. Eng. Rep.* **R33**, 1 (2001).
19. M. L. M. Balistreri, J. P. Korterik, L. Kuipers, N. F. van Hulst, *J. Lightwave Technol.* **19**, 1169 (2001).
20. Group and phase velocity of the pulse in the channel waveguide are calculated with the effective

index method. The material dispersion is taken into account as  $n^2(\lambda) = A^2 + B\lambda^2/(\lambda^2 - C^2)$ , with  $A = 0$ ,  $B = 3.8693$ , and  $C = 119.61$  nm for  $\text{Si}_3\text{N}_4$  (TM polarization) and  $A = 1$ ,  $B = 1.0998$ , and  $C =$

92.431 nm for  $\text{SiO}_2$ . The calculations use the locally measured width and height of the ridge.

21. The pulse intensities used in the experiment are low enough to prevent nonlinear processes such as self-phase modulation. As a result, the spectral content (and thus the coherence time) of the pulses does not change in either of the branches of the interferometer. Because the measurement is closely related to a field correlate, the length of the pulse as it is found inside the structure is given to first order by the coherence time of the pulse times the velocity at which the pulse travels inside the structure. These considerations lead to an expected pulse length of  $71 \pm 8$   $\mu\text{m}$ .
22. The signal in Fig. 4 is proportional to  $I(x,y) = \int dt A_{\text{sig}}(x,y,t) A_{\text{ref}}^*(t) \cos[\phi(x,y,t)]$ . Here  $A_i$  denotes the envelopes of the pulses in the signal and reference branches, and  $\phi(x,y,t)$  is the phase difference between the two branches.  $x$  and  $y$  are the coordinates along and perpendicular to the propagation direction, respectively. The reference time has been chosen so that optimal interference is achieved for  $x = 0$ . It is clear that  $I(x,y)$  has a highly similar appearance to the cross-correlation  $\Xi(\tau)$ . However, because the pulse envelope  $A_{\text{sig}}$  propagates at a different speed than the phase information,  $x$  cannot be translated to a single time delay  $\tau$ .
23. We thank K.-J. Boller, J. P. Brugger, and D. Lohse for a critical reading of the manuscript. The research described in this report is part of the Strategic Research Orientation of the MESA<sup>+</sup> Research Institute on Advanced Photonic Structures. The work was financially supported by the Dutch Foundation for Fundamental Research on Matter (FOM).

7 August 2001; accepted 4 October 2001

## Dielectrophoretic Assembly of Electrically Functional Microwires from Nanoparticle Suspensions

Kevin D. Hermanson, Simon O. Lumsdon, Jacob P. Williams, Eric W. Kaler, Orlin D. Velev\*†

A new class of microwires can be assembled by dielectrophoresis from suspensions of metallic nanoparticles. The wires are formed in the gaps between planar electrodes and can grow faster than 50 micrometers per second to lengths exceeding 5 millimeters. They have good ohmic conductance and automatically form electrical connections to conductive islands or particles. The thickness and the fractal dimension of the wires can be controlled, and composite wires with a metallic core surrounded by a latex shell can be assembled. The simple assembly process and their high surface-to-volume ratio make these structures promising for wet electronic and bioelectronic circuits.

The assembly of colloidal particles holds promise for the miniaturization of photonic and electrical circuits and their stacking in the third dimension (1, 2). Important recent de-

velopments in the field of creating miniaturized electrically functional structures include the synthesis of electronic elements by templated growth in membrane channels (3) and their assembly and characterization (4, 5), formation of electrical connections and electronic elements by electrodeposition (6, 7), and assembly of prefabricated blocks by capillary forces (8, 9). Different types of semiconductor nanowires have been synthesized by chemical or electrochemical growth (10, 11) and could be used in prototypes of elec-

Center for Molecular and Engineering Thermodynamics, Department of Chemical Engineering, University of Delaware, Newark, DE 19716, USA.

\*To whom correspondence should be addressed. E-mail: odvelev@unity.ncsu.edu

†Present address: Department of Chemical Engineering, Riddick Hall, North Carolina State University, Raleigh, NC 27695, USA.